applied sciences

IMPACT FACTOR 2.5

CITESCORE 5.3

Article

# High-Accuracy Entanglement Detection via a Convolutional Neural Network with Noise Resistance

Qian Sun, Yanyan Song, Zhichuan Liao and Nan Jiang

MDPI

https://doi.org/10.3390/app14209418

applied sciences

MDPI

*Article*

# High-Accuracy Entanglement Detection via a Convolutional Neural Network with Noise Resistance

**Qian Sun †, Yanyan Song †, Zhichuan Liao and Nan Jiang ***

School of Physics and Astronomy, Beijing Normal University, Beijing 100875, China; 202321140069@mail.bnu.edu.cn (Q.S.); 202121140060@mail.bnu.edu.cn (Y.S.); 202221140064@mail.bnu.edu.cn (Z.L.)

* Correspondence: jiangnan2019@bnu.edu.cn

† These authors contributed equally to this work.

**Abstract:** Quantum entanglement detection is one of the fundamental tasks in quantum information science. Conventional methods for quantum state tomography exhibit limitations in scalability as the number of qubits increases, leading to exponential growth in the number of unknown parameters and required measurements. Consequently, the accuracy enhancement achieved by these methods is constrained. In response to this challenge, we developed a tailored convolutional neural network (CNN) model capable of effectively detecting entanglement in two-qubit quantum states, achieving an accuracy exceeding 97.5%. Notably, even in the presence of noise, this model retains its robust performance, displaying resilience against a tolerable level of noise contamination. Furthermore, the inherent generalization power of CNNs allows our model, which was initially trained on a specific spectrum of quantum states, to extend its applicability to wider states, positioning it as an outstanding tool for the further application of machine learning in the field of quantum computing, opening up new pathways for solving entanglement detection problems in quantum information.

**Keywords:** entanglement detection; quantum state tomography; neural network; noise resistance; generalization



**Citation:** Sun, Q.; Song, Y.; Liao, Z.; Jiang, N. High-Accuracy Entanglement Detection via a Convolutional Neural Network with Noise Resistance. *Appl. Sci.* **2024**, *14*, 9418. https://doi.org/10.3390/app14209418

Academic Editor: Augusto Ferrante

Received: 24 September 2024
Revised: 11 October 2024
Accepted: 13 October 2024
Published: 16 October 2024



## 1. Introduction

Quantum entanglement empowers qubits [1] to encode and manipulate a huge amount of data within superposed states, surpassing the limitations inherent in classical computational models [2]. However, identifying entanglement poses a highly challenging problem [2–4], primarily due to the intricate nature of quantum correlations. The gold standard for entanglement detection is comprehensive quantum state tomography [5], which offers high fidelity but becomes prohibitively resource-intensive as the quantum system scales up. This exponential growth in the number of accessible states and the dimensionality of the Hilbert space underscores the need for alternative approaches. In scenarios where full state information is inaccessible, there arises a demand for direct classification of entanglement based on incomplete or partial knowledge of the underlying quantum state. This paradigm shift necessitates the development of efficient methods that can discern entanglement patterns even with limited data [6–9]. Furthermore, noise introduces a significant impediment to entanglement detection by disrupting the precise identification and manipulation of quantum states. The detrimental effects of noise manifest as interference during the quantum state analysis process, underscoring the importance of noise-resilient detection strategies to mitigate these challenges [10]. The pursuit of such advanced techniques is crucial for advancing the field of quantum information processing and enabling the practical implementation of large-scale, fault-tolerant quantum computers.

In recent years, machine learning has become a crucial tool for solving high-complexity problems in physics [11], particularly when dealing with hierarchically structured and spatially correlated data [12–14]. More specifically, machine learning has also been widely

applied in the field of quantum technology, such as combining reinforcement learning methods for quantum control [15–17]. Convolutional neural network (CNN) is a typical supervised learning algorithm proposed by LeCun in 1998 [18] and widely used in various data processing tasks. The supervised learning refers to using samples $\mathbf{X}_i$ with target labels $\mathbf{Y}_i$ to train a model. During the training progress, the update rate of the parameters is adjusted based on the difference between the predicted value $\mathbf{Y}'_i$ and the target value $\mathbf{Y}_i$ to make the model fit the training data more accurately, and the difference is usually defined as the loss function of supervised learning. Compared to fully connected neural network architectures, CNNs use weight sharing and local connections as their main strategies, and can reduce the dimensionality of data as needed, which increase the speed of network training and mitigate the problem of overfitting to some extent, thus enhancing the model's generalization [18,19]. Additionally, during the training process, the method of batch normalization can be introduced to improve training accuracy and speed [20], and an orthonormal basis can be created in the latent space of CNNs to avoid overfitting and other learning pathologies associated with correlated attributions to dimensions of the latent space [21]. CNNs can effectively process and analyze complex data from simulations or experimental measurements in many-body quantum systems [22]. A CNN-based scheme for quantum state tomography outperforms traditional techniques in terms of fidelity and accuracy of observable estimation [23]. CNNs primarily distinguish between different quantum states by learning from data obtained through quantum measurements for quantum state classification purposes [24]. Therefore, the CNN-based approach holds promise for discriminating between entangled and separable states in quantum information processing.

Noise is a pervasive phenomenon in quantum information processing and quantum computing, which poses a formidable challenge to the realization of reliable and efficient quantum systems. Due to the high sensitivity of quantum systems and the fragility of quantum states, noise can lead to significant information loss and computational errors [25,26]. Moreover, even minuscule amounts of noise can have a disproportionately large impact on the system's performance. Therefore, effectively managing and combating noise is one of the core challenges in achieving reliable quantum computing and quantum communication technologies. The sources of noise are diverse, ranging from fluctuations in the environment to imperfections in hardware components and imprecise measurements. Currently, various advanced statistical methods have been applied to QST, such as Bayesian inference, variational quantum eigensolver, and quantum neural networks, which alleviate the problems of noise handling and low computational efficiency in traditional linear inversion and maximum likelihood estimators [27].

Given their robustness in handling noisy image and signal processing [28], the exploration of CNNs for quantum state classification represents an exciting avenue of research. They can perform more accurate classifications by extracting characteristic patterns from noisy data, although they still face challenges in high-noise environments. In this paper, we primarily focus on the entanglement characteristics of quantum states by simplifying the regression task of quantum state tomography (QST) into a classification problem. While improving computational efficiency, we achieve good resistance to noise by leveraging the inherent generalization capabilities of CNNs. Furthermore, we can maintain considerable noise resilience while reducing the number of measurement operators that relate to the information we can obtain. The results show that the model achieves an accuracy rate exceeding 97.5% in determining entanglement for two-qubit quantum states in the absence of noise, and it also exhibits resilience to a specific degree of noise interference.

## 2. Methods

### 2.1. Basic Idea

In quantum physics, a pure state system is considered separable if it can be expressed as the tensor product of the states of two subsystems. This description can be extended to the framework of density matrices to handle mixed states. Mixed states need to be expressed as a convex combination of separable states [29,30]. In contrast, a composite

system in an entangled state indicates a nonclassical, strong correlation between its two subsystems. When systems A and B are entangled, measurements on A inevitably affect B, causing quantum state collapse. To ensure the reliability of classification, the training CNN model follows the main principle outlined below:

The input data for the training set consist of probabilities, which are computed using Born's rule applied to a specified set of known density matrices $\rho$ and operators $\{\mathbf{O}_k\}$. These probabilities reflect the likelihoods of the corresponding measurement outcomes. In short, the model learns from these probability distributions to identify the properties of quantum states, particularly distinguishing separable states from entangled states.

In addressing the discrimination in two-qubit systems, we adopt the positive partial transpose (PPT) criterion [31,32] as a rigorous standard to segregate quantum states into entangled and separable categories. The density matrix $\rho$ is deemed to represent an entangled state if its partial transpose matrix possesses at least one negative eigenvalue. On the contrary, if no negative eigenvalues are encountered in the partial transpose, $\rho$ is classified as a separable state. Once the PPT criterion has been applied to assign categorical labels, we establish a mathematical convention of representing separable states with '1' and entangled states with '2', as illustrated in Figure 1. After rigorous training, the neural network processes measurement frequencies of unknown quantum states and outputs their classification as entangled or separable. Reliability depends on network architecture, training rigor, and dataset quality.

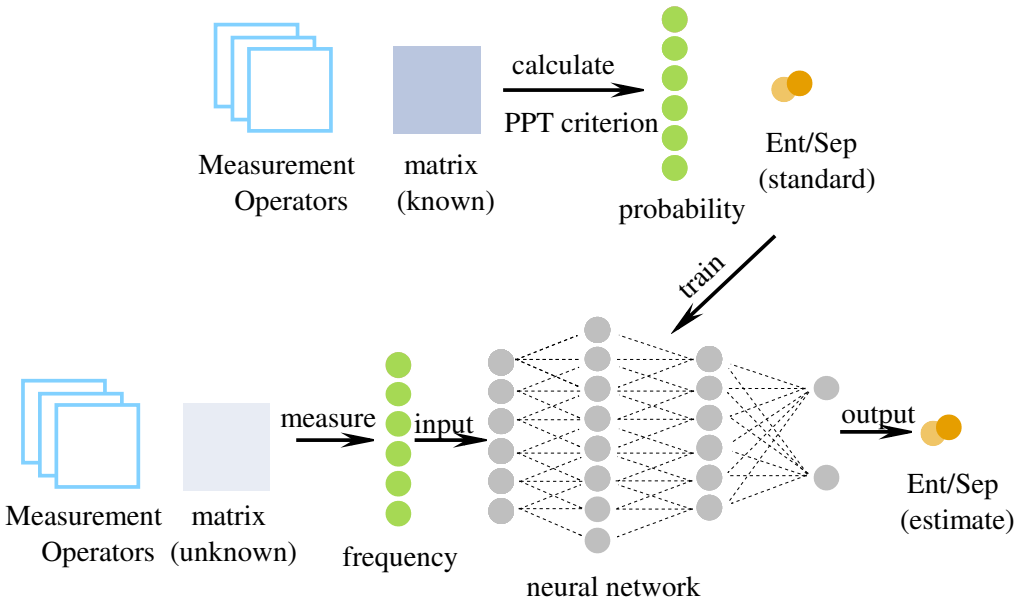


**Figure 1.** The basic idea of using deep neural networks to implement entanglement detection.

To facilitate this classification, we randomly generate multiple sets of predefined density matrices $\rho$, and calculate the probability $P = Tr(\rho\mathbf{O}_k)$ with distinct measurement operators $\{\mathbf{O}_k\}$ as the input dataset. Subsequently, we apply the PPT criterion to these inputs, generating the corresponding labels as our output dataset, which serve as the foundation for training our model.

For binary classification, according to the estimated results and true labels, there are four situations in total: true positive (TP), false positive (FP), true negative (TN), and false negative (FN). The results can be evaluated by accuracy, precision, and recall as follows:

$$Accuracy = \frac{TP + TN}{TP + TN + FP + FN}, \tag{1}$$

$$Precision = \frac{TP}{TP + FP}, \tag{2}$$

and

$$Recall = \frac{TP}{TP + FN}. \tag{3}$$

The accuracy represents the proportion of correctly classified samples out of all samples, while the precision measures the proportion of true positive examples among all samples classified as positive. A higher precision indicates a lower likelihood of misclassifying negative examples as positive. On the other hand, the recall is the ratio of successful detections among all true positives. A higher recall rate implies fewer missed positive examples.

### *2.2. Noise Models*

Pauli noise is a comprehensive noise model that includes Pauli matrices $(\sigma_x, \sigma_y, \sigma_z)$, representing quantum bit flipping, simultaneous bit and phase flipping, and phase flipping, respectively. In quantum systems, this type of noise can cause errors in the state of quantum bits, ranging from simple flipping to more complex errors. In a two-qubit system, qubit Pauli noise is defined as [33]

$$\epsilon(\rho) = (1 - \varepsilon)\rho + \varepsilon \sum_{k=1}^{16} p_k (\sigma_{1,i} \otimes \sigma_{2,j}) \rho (\sigma_{1,i} \otimes \sigma_{2,j})^\dagger. \tag{4}$$

In this model, $\rho$ represents the initial density matrices of the two-qubit quantum state. $\varepsilon$ is a parameter characterizing the intensity of the noise, with a value ranging between 0 and 1. $\sigma_{1,i} \otimes \sigma_{2,j}$ denotes the combination of Pauli operations (including an additional $2 \times 2$ identity matrix $\mathbf{I}$) applied to the two qubits, where $\sigma_{1,i}$ and $\sigma_{2,j}$ are Pauli operators acting on the first and second qubit, respectively. $k$ represents the probability distribution for the $k^{th}$ combination of operations, satisfying $\sum_{k=1}^{16} p_k = 1$ to ensure the completeness of probabilities. To simplify our analysis, we opted for the basic formula,

$$\epsilon(\rho) = (1 - \varepsilon)\rho + \varepsilon(\mathbf{I} \otimes \sigma_{2,x}) \rho (\mathbf{I} \otimes \sigma_{2,x})^\dagger, \tag{5}$$

and it is worth noting that other forms can adhere to the same logical framework as well.

Depolarizing noise causes a quantum bit to gradually lose its specific state, transitioning toward a completely mixed state. Depolarizing noise makes the information in a quantum bit more random. The formula for two-qubit depolarizing noise is

$$\epsilon(\rho) = (1 - \varepsilon)\rho + \frac{\varepsilon \mathbf{I}}{4}, \tag{6}$$

and the definitions of each parameter are consistent with those previously mentioned.

Dephasing noise primarily affects the phase of a quantum bit rather than its amplitude. Phase damping does not change the probabilities of the qubit being in $|0\rangle$ and $|1\rangle$ but causes changes in their phase relationships. In a two-qubit system, dephasing noise is given by

$$\epsilon(\rho) = (1 - \varepsilon)\rho + \frac{\varepsilon}{2}((\sigma_z \otimes \mathbf{I})\rho(\sigma_z \otimes \mathbf{I})^\dagger + (\mathbf{I} \otimes \sigma_z)\rho(\mathbf{I} \otimes \sigma_z))^\dagger. \tag{7}$$

Amplitude-damping noise is often associated with energy loss, such as the transition of a quantum bit from an excited state to a ground state. This type of noise is particularly common in quantum optical systems, where quantum bits lose energy through interactions with the environment. Amplitude-damping noise is defined with the Kraus operator. $\mathbf{E}_0 = |0\rangle\langle 0| + \sqrt{1 - \varepsilon}|1\rangle\langle 1|$ and $\mathbf{E}_1 = \sqrt{\varepsilon}\,|0\rangle\langle 1|$. Its operator-sum representation can be expressed as

$$\epsilon(\rho) = \mathbf{E}_0 \rho \mathbf{E}_0^\dagger + \mathbf{E}_1 \rho \mathbf{E}_1^\dagger. \tag{8}$$

The four noise models enable us to simulate the detrimental effects of noise by mixing the original quantum state with its counterparts that have undergone diverse Pauli

transformations, where the noise intensity is governed by the parameter $\varepsilon$. By meticulously adjusting both the $\varepsilon$ value and the probabilities $p_k$ associated with each specific combination of Pauli operations $\sigma_{1,i} \otimes \sigma_{2,j}$, we can thoroughly analyze the evolution of the quantum state under a given noise scenario. These noise models mentioned are then applied directly to the density matrices, enabling us to quantify the influence of noise, and, consequently, simulate its implications on the performance of entanglement detection utilizing CNNs. This approach provides insights into the robustness of entanglement detection in the presence of various noise scenarios.

### *2.3. CNN Training*

We use Werner states as follows to implement the network training and entanglement detection:

$$\rho = p|\psi\rangle\langle\psi| + \frac{1-p}{4}\mathbf{I}, \tag{9}$$

here $|\psi\rangle = \frac{\sqrt{2}}{2}(|10\rangle - |01\rangle)$, $p \in (0,1)$, and $\mathbf{I}$ represents the $2 \times 2$ identity matrix.

We implement entanglement detection with a CNN constructed by the Deep Learning Toolbox of MATLAB. The networks' hidden layers include two convolution layers activated by the leaky rectified linear unit (ReLU) function, two max-pooling layers, and one fully connected layer, and the softmax function is used to activate the output layer. The specific architecture and hyperparameters used in our neural network training are detailed in Tables 1 and 2. This information is crucial for understanding and replicating our experimental results.

**Table 1.** The structure of our model.

| | **Complete Measurement** | **Incomplete Measurement** |
|---|---|---|
| **Image Input Layer** | $16 \times 1 \times 1$ | $4 \times 1 \times 1$ |
| Input channels | 1 | 1 |
| **2D-Convolution Layer** | | |
| Input channels | 1 | 1 |
| Kernel | $2 \times 1$ | $1 \times 1$ |
| Stride | 1, No Padding | 1, NO Padding |
| Output channels | 8 | 8 |
| Activation function | leakyReLU ($\alpha = 0.01$) | leakyReLU ($\alpha = 0.01$) |
| **Max-Pooling Layer** | | |
| Input channels | 8 | 8 |
| Kernel | $2 \times 1$ | $1 \times 1$ |
| Stride | 2, No Padding | 1, NO Padding |
| Output channels | 8 | 8 |
| **2D-Convolution Layer** | | |
| Input channels | 8 | 8 |
| Kernel | $2 \times 1$ | $2 \times 1$ |
| Stride | 1, No Padding | 1, NO Padding |
| Output channels | 16 | 16 |
| Activation function | leakyReLU ($\alpha = 0.01$) | leakyReLU ($\alpha = 0.01$) |
| **Max-Pooling Layer** | | |
| Input channels | 16 | 16 |
| Kernel | $2 \times 1$ | $2 \times 1$ |
| Stride | 2, No Padding | 1, NO Padding |
| Output channels | 16 | 16 |
| **Fully-Connected Layer** | | |
| Units | 2 | 2 |
| **Classification Output Layer** | | |
| Activation function | Softmax | Softmax |
| Loss function | Crossentropy | Crossentropy |

**Table 2.** The hyperparameters of our model.

| Parameters | Value |
|---|---|
| Optimizer | Adam |
| Initial Learning Rate | 0.01 |
| Mini Batch Size | 6000 |
| Max Epochs | 800 |

The positive examples considered include entangled states and separable states, which are characterized by five indices: accuracy (Acc), the precision of entangled states (Pre-Ent), the precision of separable states (Pre-Sep), the recall of entangled states (Rec-Ent), and the recall of separable states (Rec-Sep).

## 3. Results

### *3.1. Entanglement Detection without Noise*

Using the corresponding measured frequencies as input dataset, our trained model will output corresponding detection results, with labels '1' and '2' representing separable and entangled states respectively, which is the same as previously stipulated. The measurement is conducted on 100,000 randomly generated density matrices. Using the probability $P = Tr(\rho \mathbf{O_k})$, the measurement process without additional interference is simulated with the Monte Carlo method and logical operation. The number of random numbers generated can be adjusted to vary the number of simulated measurement operations.

A minimum of 15 parameters are needed to determine a two-qubit density matrix completely, known as complete measurement [1]. To optimize resource utilization and improve efficiency, we aim to manipulate incomplete measurements for reliable results. In our work, we initially employ 16 optical polarization operators with an additional one ensuring measurement completeness.

When simulating incomplete measurement, we gradually eliminate the aforementioned complete measurement operators. Finally, for the specific random states of interest, we reduce the number of operators to 4 as listed below:

$$\begin{aligned} \mathbf{O_1} &= |00\rangle\langle 00|; \\ \mathbf{O_2} &= |01\rangle\langle 01|; \\ \mathbf{O_3} &= |10\rangle\langle 10|; \\ \mathbf{O_4} &= |11\rangle\langle 11|. \end{aligned} \tag{10}$$

The models' computation time is shown in Table 3 and the classification results without noise are shown in Figure 2. Except for the Rec-Sep, which is slightly lower than that of the other indicators when measured 1000 times, all the judgment indicators exceed 97.5%. This classification model performs well without noise.

**Table 3.** Model's computation time.

| | Classification Time | Training Time |
|---|---|---|
| Complete measurement | 0.003249 s | 1 min 50 s |
| Incomplete measurement | 0.002577 s | 1 min 47 s |

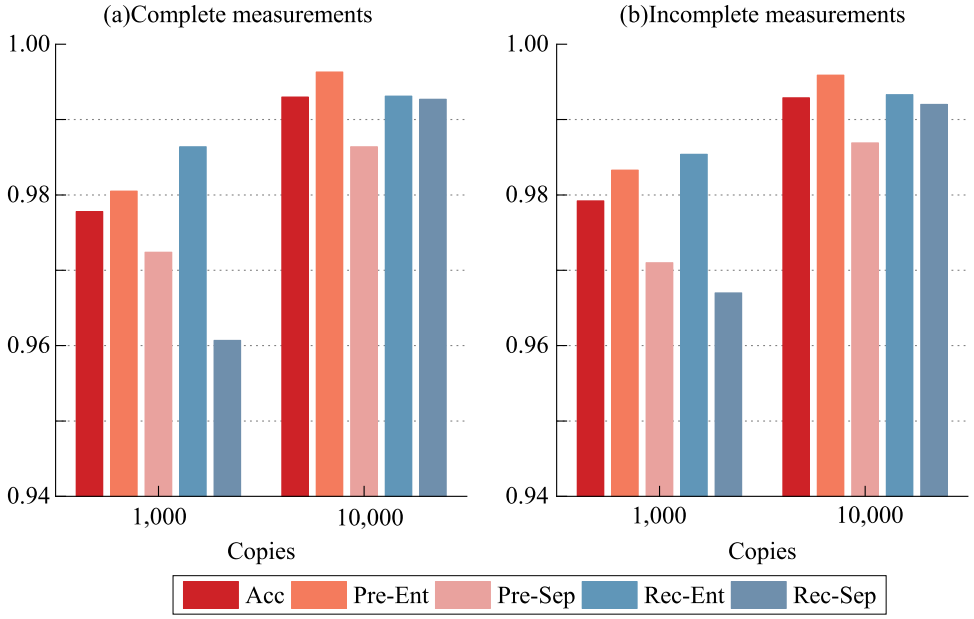


**Figure 2.** Results of entanglement detection without noise. The accuracy of both complete and incomplete measurements exceeded 97.5%, and the precision and recall exceeded 96%. Under 10,000 simulated measurements, the accuracy increased to over 99%, and both the precision and recall exceeded 98%. (**a**) Result of the complete measurement. (**b**) Result of the incomplete measurements obtained by 4 measurement operators.

### *3.2. Demonstration of Robust Performance in the Presence of Noise*

To simulate the detection under the influence of noise, we apply the operations shown in Equations (5)–(8) to randomly generate density matrices after obtaining the labels by PPT criterion. Then, we conduct complete or incomplete measurements on the processed matrices and feed the resulting data into the trained model previously. Finally, we compare the output results with the standard labels while applying four types of noise models to the measured state and increasing the error rate $\varepsilon$. The results under both complete and incomplete measurements are shown in Figure 3 and Figure 4, respectively.

This classification model tends to classify more states as the same type of state (separable or entangled states) under high error rates, which will result in a decrease in the recall for one type of quantum state and an increase in another's precision at meantime, with the overall accuracy decreasing. The classification model gradually deteriorates under the influence of noise. When the error rate is not excessively high, the generalization of CNNs ensures our models' high resistance to noise impact. As shown in Figure 3, when conducting complete measurement, for depolarizing noise, dephasing noise, and amplitude damping noise, the accuracy only dropped by less than 2% even with an error rate $\varepsilon$ of 20%.

In Figure 4, for incomplete measurement with a raised error rate of 10%, the accuracy dropped by less than 5% under four types of noise influence. Due to measurement incompleteness, less information about the density matrices can be determined, resulting in lower resistance to noise compared to complete measurement.

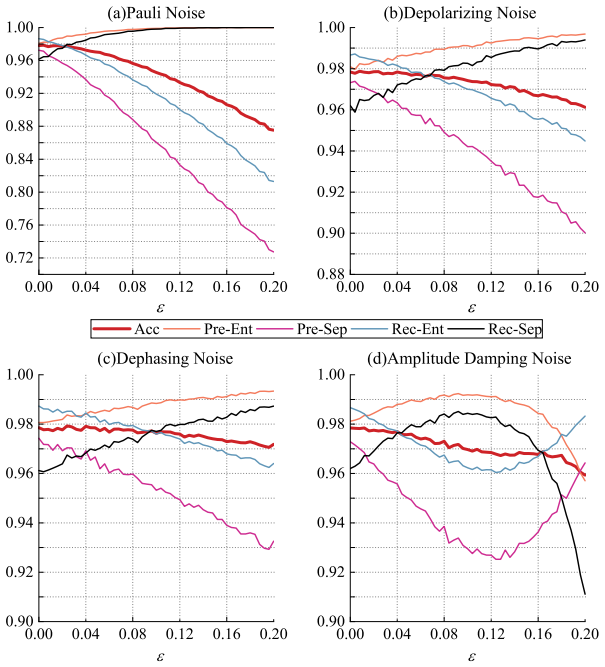


**Figure 3.** Complete measurement results with four types of noise models, where ε represents the error rate, increasing from 0 to 0.2. Except for Pauli noise, the decrease in accuracy under the other noise models is less than 2%.

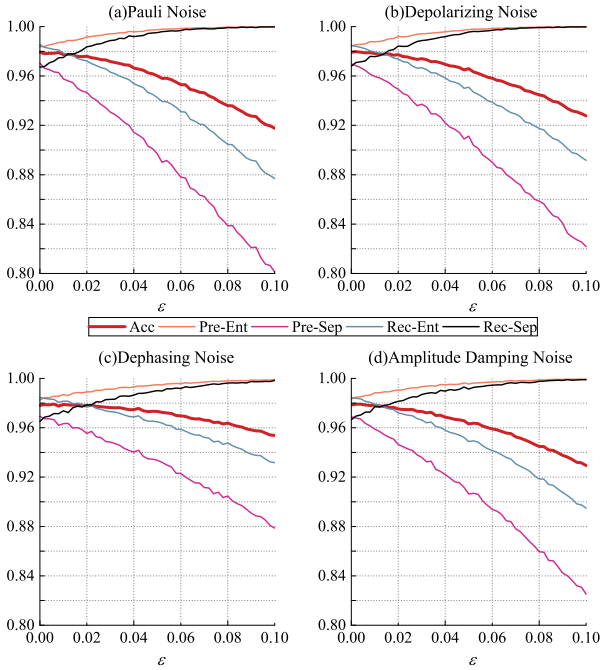


**Figure 4.** Incomplete measurement results with four types of noise models, where ε represents the error rate. The error rate increases from 0 to 0.1, with the accuracy decreasing by about 5% under the four types of noise.

### *3.3. The Generalization of Our Classification Model*

The resistance of this classification model is related to the generalization of the CNN to a certain extent, which generally refers to the situation in which the training dataset differs from the testing dataset. Generalization is a fundamental metric that assesses a model's capability to learn general patterns from training data and successfully apply them to new,

unseen data. In the context of CNNs, the max pooling layer serves as a vital component, playing a pivotal role in enhancing the model's generalization. By adopting the strategy of selecting the maximum value within a local region as the output, max pooling effectively reduces the dimensionality of feature maps, decreases the computational complexity of the model, and simultaneously strengthens its robustness against minor variations in input data. This local invariance enables the model to enhance its generalization.

In the case of the aforementioned results, we employ a randomized sampling approach to procure our datasets, ensuring that there is a minimal chance of direct overlap between the training dataset and testing dataset. This strategy inherently promotes a scenario where the model is tested on data that are genuinely novel and unseen during the training process. Consequently, the foundation for the model's generalization is firmly established and validated, as it demonstrates its ability to adapt and apply learned patterns to dissimilar data instances, thereby reinforcing its capacity to generalize effectively.

Here, we proceed to validate the model's generalization capability through testing. We still use the network above trained with random states $\rho = p|\psi\rangle\langle\psi| + \frac{1-p}{4}\mathbf{I}$; here, $|\psi\rangle = \frac{\sqrt{2}}{2}(|01\rangle - |10\rangle)$. We change to obtain the testing set from $|\psi\rangle = \frac{\sqrt{2}}{2}(|01\rangle + |10\rangle)$, $\frac{\sqrt{2}}{2}(|00\rangle - |11\rangle)$, or $\frac{\sqrt{2}}{2}(|00\rangle + |11\rangle)$. The comparison results are shown in Figure 5. When changing within a certain range, the classification model can still achieve good performance.

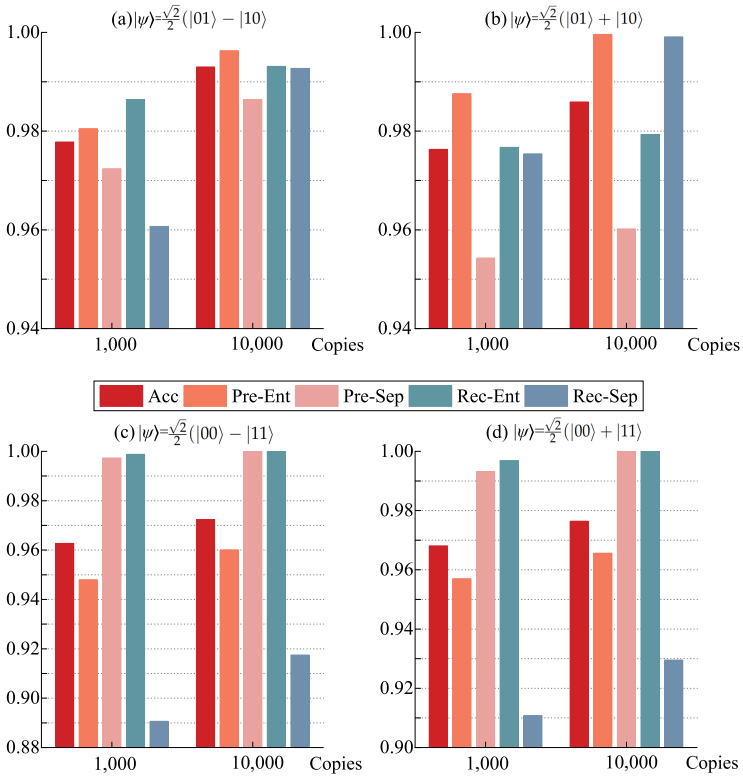


**Figure 5.** Detection results for other ranges of quantum states. The testing dataset is expanded to different ranges of state $|\psi\rangle$.

For states $|\psi\rangle = \frac{\sqrt{2}}{2}(|01\rangle + |10\rangle)$, the accuracy is almost the same as the testing dataset $|\psi\rangle = \frac{\sqrt{2}}{2}(|01\rangle - |10\rangle)$ similar to the training dataset with the measurements repeated 1000 times, and decreases from 99.30% to 98.59% in 10,000 repeated measurements. Although the accuracy decreases even further when the testing dataset is expanded to $|\psi\rangle = \frac{\sqrt{2}}{2}(|00\rangle \pm |11\rangle)$, the accuracies exceed 96% and 97% in repeated measurements of 1000 and 10,000, respectively, indicating that our model's generalization is relatively reliable.

## 4. Discussion

In this work, we employed the impressive recognition and generalization of convolution neural networks for complex multidimensional data to implement entanglement detection. This classification model achieved an accuracy exceeding 97.5%, making it a reliable tool for determining entanglement solely based on measurement results, without requiring complete information about the quantum states. Despite the impact of noise, this classification model maintains its excellent performance, demonstrating resilience against a certain degree of noise influence. Additionally, the generalization of convolutional neural networks enables this classification model, which was trained on a certain range of quantum states, to a certain extent, to extend to different states, making it an exceptional tool for entanglement detection. The model schemes hold great potential for future applications in the field of entanglement detection, and we are exploring optimization schemes to make the model more effective to higher dimensional systems. Furthermore, although our model has yielded positive results, we recognize that the quantum states we are currently studying have relatively simple density matrix forms. In future research, we can further consider improving the model structure or mixing noisy samples into the training data, aiming to enhance the performance of this noise-resistant model in handling quantum states with greater randomness and expand its applicability.

**Author Contributions:** Conceptualization, Y.S. and Q.S.; methodology, Q.S. and Z.L.; software, Q.S.; formal analysis, Q.S. and Y.S.; data curation, Y.S.; writing—original draft preparation, Q.S. and Y.S.; writing—review and editing, Z.L. and N.J.; supervision, N.J.; project administration, N.J.; funding acquisition, N.J. All authors have read and agreed to the published version of the manuscript.

**Funding:** This research was funded by National Natural Science Foundation of China grant number 12204055 and Fundamental Research Funds for the Central Universities grant number 2243100012.

**Institutional Review Board Statement:** Not applicable.

**Informed Consent Statement:** Not applicable.

**Data Availability Statement:** The data presented in this study are available from the corresponding author on reasonable request due to privacy protection concerns.

**Acknowledgments:** We would like to thank Xiaobo Chen at Beijing Normal University, who provided some space for this research.

**Conflicts of Interest:** The authors declare no conflicts of interest.

## Abbreviations

The following abbreviations are used in this manuscript:

| | |
|---|---|
| CNN | Convolutional neural network |
| PPT | Positive partial transpose |
| TP | True positive |
| FP | False positive |
| TN | True negative |
| FN | False negative |
| ReLU | Rectified linear unit |
| Acc | Accuracy |
| Pre-Ent | Precision of entangled states |
| Pre-Sep | Precision of separable states |
| Rec-Ent | Recall of entangled states |
| Rec-Sep | Recall of separable states |

## References

1. James, D.F.V.; Kwiat, P.G.; Munro, W.J.; White, A.G. Measurement of qubits. *Phys. Rev. A* **2001**, *15*, 052312. [CrossRef]
2. Asif, N.; Khalid, U.; Khan, A.; Duong, T.Q.; Shin, H. Entanglement detection with artificial neural networks. *Sci. Rep.* **2023**, *13*, 1562. [CrossRef] [PubMed]
3. Toth, G.; Guehne, O. Entanglement detection in the stabilizer formalism. *Phys. Rev. A* **2005**, *72*, 22340–22353. [CrossRef]

4. Zhao, Y.Y.; Xiang, G.Y.; Hu, X.M.; Liu, B.H.; Li, C.F.; Guo, G.C.; Schwonnek, R.; Wolf, R. Entanglement detection by biolations of noisy uncertainty relations: A proof of principle. *Phys. Rev. Lett.* **2019**, *122*, 220401. [CrossRef]
5. Vogel, K.; Risken, H. Determination of quasiprobability distributions in terms of probability distributions for the rotated quadrature phase. *Phys. Rev. A* **1989**, *40*, 2847–2849. [CrossRef]
6. Cillian, H.; Mauro, P.; Stefano, P. Mixed state entanglement classification using artificial neural networks. *New J. Phys.* **2021**, *23*, 063033.
7. Torlai, G.; Mazzola, G.; Carrasquilla, J.; Troyer, M.; Melko, R.; Carleo, G. Neural-network quantum state tomography. *Nat. Phys.* **2018**, *14*, 447–450. [CrossRef]
8. Cramer, M.; Plenio, M.B.; Flammia, S.T.; Somma, R.; Liu, Y.K. Efficient quantum state tomography. *Nat. Commun.* **2010**, *1*, 149–155. [CrossRef]
9. Clerk, A.A.; Devoret, M.H.; Girvin, S.M.; Marquardt, F.; Schoelkopf, R.J. Introduction to quantum noise, measurement, and amplification. *Rev. Mod. Phys.* **2010**, *82*, 1155–1208. [CrossRef]
10. Nguyen, N.H.; Behrman, E.C.; Steck, J.E. Quantum learning with noise and decoherence: A robust quantum neural network. *Quantum Mach. Intell.* **2020**, *2*, 1. [CrossRef]
11. Vedran, D.; Hans, J.B. Machine learning & artificial intelligence in the quantum domain: A review of recent progress. *Rep. Prog. Phys.* **2018**, *81*, 074001.
12. Hinton, G.E.; Salakhutdinov, R.R. Reducing the dimensionality of data with neural networks. *Science* **2006**, *313*, 504–507. [CrossRef] [PubMed]
13. Wang, L. Discovering phase transitions with unsupervised learning. *Phys. Rev. B* **2016**, *94*, 195105–195109. [CrossRef]
14. Carleo, G.; Cirac, I.; Cranmer, K.; Daudet, L.; Schuld, M.; Tishby, N.; Vogt-Maranto, L.; Zdeborová, L. Machine learning and the physical sciences. *Rev. Mod. Phys.* **2019**, *91*, 45002–45040. [CrossRef]
15. Bukov, M.; Day, A.G.; Sels, D.; Weinberg, P.; Polkovnikov, A.; Mehta, P. Reinforcement learning in different phases of quantum-control. *Phys. Rev. X* **2018**, *8*, 031086.
16. Zhang, X.M.; Wei, Z.; Asad, R.; Yang, X.C.; Wang, X. When doesreinforcement learning stand out in quantum control? Acomparative study on state preparation. *NPJ Quantum Inf.* **2019**, *5*, 8. [CrossRef]
17. Yu, H.; Zhao, X. Deep Reinforcement Learning with RewardDesign for Quantum Control. *IEEE Trans. Artif. Intell.* **2024**, *5*, 1087–1101. [CrossRef]
18. Lecun, Y.; Bottou, L.; Bengio, Y.; Haffner, P.Y. Gradient-based learning applied to document recognition. *Proc. IEEE* **1998**, *86*, 2278–2324. [CrossRef]
19. Simonyan, K.; Zisserman, A. Very deep convolutional networks for large-scale image recognition. *arXiv* **2014**, arXiv:1409.1556.
20. Ioffe, S.; Szegedy, C. Batch normalization: Accelerating deep network training by reducing internal covariate shift. *arXiv* **2015**, arXiv:1502.03167v3.
21. Flouris, K.; Konukoglu, E. Canonical normalizing flows for manifold learning. *NIPS* **2023**, *36*, 27294–27314.
22. Carleo, G.; Troyer, M. Solving the quantum many-body problem with artificial neural networks. *Science* **2016**, *355*, 602–606. [CrossRef]
23. Schmale, T.; Reh, M.; Gaerttner, M. Efficient quantum state tomography with convolutional neural networks. *NPJ Quantum Inf.* **2022**, *8*, 115. [CrossRef]
24. Kookani, A.; Mafi, Y.; Kazemikhah, P.; Aghababa, H.; Fouladi, K.; Barati, M. XpookyNet: Advancement in quantum system analysis through convolutional neural networks for detection of entanglement. *Quantum Mach. Intell.* **2024**, *6*, 50. [CrossRef]
25. Schindler, P.; Barreiro, J.T.; Monz, T.; Nebendahl, V.; Nigg, D.; Chwalla, M.; Hennrich, M.; Blatt, R. Experimental repetitive quantum error correction. *Science* **2011**, *332*, 1059–1061. [CrossRef] [PubMed]
26. Córcoles, A.D.; Magesan, E.; Srinivasan, S.J.; Cross, A.W.; Steffen, M.; Gambetta, J.M.; Chow, J.M. Demonstration of a quantum error detection code using a square lattice of four superconducting qubits. *Nat. Commun.* **2015**, *6*, 6979–6988. [CrossRef] [PubMed]
27. Archpaul, J.; VijayaKumar, E.N.; Rajendran, M.; Stephan, T.; Stephan, P.; Chhabra, R.; Agarwal, S.; Pak, W. Enhancing quantum state tomography: Utilizing advanced statistical techniques for optimized quantum state reconstructions. *J. Korean Phys. Soc.* **2024**, *85*, 677–690. [CrossRef]
28. Sajedian, I.; Kim, J.; Rho, J. Finding the optical properties of plasmonic structures by image processing using a combination of convolutional neural networks and recurrent neural networks. *Microsyst. Nanoeng.* **2019**, *5*, 27. [CrossRef]
29. Ma, Y.C.; Yung, M.H. Transforming Bell's inequalities into state classifiers with machine learning. *NPJ Quantum Inf.* **2019**, *4*, 34. [CrossRef]
30. Horodecki, P. Separability criterion and inseparable mixed states with positive partial transposition. *Phys. Rev. A* **1997**, *232*, 333–339. [CrossRef]
31. Horodecki, R.; Horodecki, P.; Horodecki, M.; Horodecki, K. Quantum entanglement. *Rev. Mod. Phys.* **2009**, *81*, 865–942. [CrossRef]
32. Peres, A. Separability criterion for density matrices. *Phys. Rev. Lett.* **1996**, *77*, 1413–1415. [CrossRef] [PubMed]
33. Guo, Y.; Yang, S. Noise effects on purity and quantum entanglement in terms of physical implementabilit. *NPJ Quantum Inf.* **2023**, *9*, 11. [CrossRef]